RIG-I and MDA5 cooperatively recognize the DENV replicative-form dsRNA to activate innate immunity

Sichao Ye[1,2], Yisha Liang[1,2,3], Yu Chang[3], Bailiang Lai[1,2], Jin Zhong[1,2,3#]

[1] CAS Key Laboratory of Molecular Virology and Immunology, Shanghai Institute of Immunity and Infection, Chinese Academy of Sciences, Shanghai 200031, China.

[2] University of Chinese Academy of Sciences, Beijing 100049, China.

[3] ShanghaiTech University, Shanghai 201210, China.

#Correspondence: E-mail: jzhong@ips.ac.cn, Shanghai Institute of Immunity and Infection, Chinese Academy of Sciences, 320 Yueyang Road, Shanghai, 200031, China.

Phone: (86) 21-54923143. Fax: (86) 21-54923142.

Abstract

RIG-I like receptors (RLRs) are a family of cytosolic RNA sensors that sense RNA virus infection to activate innate immune response. It is generally believed that different RNA viruses are recognized by either RIG-I or MDA5, two important RLR members, depending on the nature of pathogen-associated molecular patterns (PAMPs) that are generated during RNA virus infection. However, it remains elusive which RLR is involved in sensing the PAMPs of Dengue virus (DENV), an important RNA virus causing serious human diseases, and the molecular basis of the DENV PAMPs is poorly defined. Here, we demonstrated that the DENV infection-induced interferon response is dependent upon both RIG-I and MDA5, with RIG-I playing a predominant role. Next we purified the DENV PAMPs from the DENV-infected cells by biochemical approaches and demonstrated that the purified DENV PAMPs are viral full-length double-stranded RNA bearing 5'ppp modifications, likely representing the viral replicative-form RNA. Finally, we confirmed the nature of the DENV PAMPs by reconstituting the viral replicative-form RNA from *in vitro* synthesized DENV genomic RNA. In conclusion, our work defined the molecular basis of the RLR-PAMP interactions during DENV infection, and revealed the previously neglected cooperative contributions by different RLRs in innate immunity against RNA viruses.

Author summary

The molecular interaction between PAMPs and RLRs plays a crucial role in innate immune response against the RNA virus infection. To our knowledge, it remains an open question which RLR member (RIG-I or MDA5) is involved in sensing DENV PAMPs, and the exact molecular basis of the DENV PAMPs is poorly defined. In this study, we demonstrated that both RIG-I and MDA5 are involved in sensing the DENV infection, with RIG-I playing a predominant role. Furthermore, we demonstrated that the DENV PAMPs is likely DENV replicative-form RNA, a double-stranded RNA bearing 5'ppp modification. Our work not only clarified which RLR and what viral PAMPs are involved in innate immune sensing of DENV infection, but also revealed previously underappreciated synergistic contributions by different RLRs in innate immunity against RNA viruses.

Introduction

Dengue virus (DENV) belongs to the family *Flaviviridae*, genus *Flavivirus*, and exists as four antigenically distinct serotypes (denoted DENV1–4)[1]. DENV is predominantly transmitted through bites of female mosquitoes *Aedes aegypti* and *Aedes albopictus*, and is recognized as one of the most severe arboviral infections around the world[2]. Approximately half of the global population is currently at risk of DENA infection, with about 100 to 400 million infections occurring annually. DENV infection causes a wide spectrum of diseases, ranging from asymptomatic infections to febrile illnesses, and potentially progressing to life-threatening dengue hemorrhagic fever and dengue shock syndrome[3].

DENV is a positive (+) strand RNA virus. The 10.7-kb RNA genome consists of a capped 5' untranslated region (5'UTR), a single open reading frame (ORF), and a 3'UTR[4]. The viral ORF is translated into a polyprotein, which is then processed to individual proteins including three structural proteins (C, precursor membrane (prM), and E) as well as seven non-structural proteins (NS1, NS2A, NS2B, NS3, NS4A, NS4B, and NS5)[5]. The DENV entry is achieved through receptor-mediated endocytosis. Upon the fusion of viral envelope and endosomal membrane, the DENV nucleocapsid disassembles to release the viral genomic RNA into the cytoplasm. The viral genomic RNA serves as the mRNA template for the synthesis of viral proteins. The viral RNA-dependent RNA polymerase (NS5) replicates the viral RNA genome within replication complexes formed on the endoplasmic reticulum membrane[6]. Throughout this intricate process, multiple forms of viral RNA are generated. The genomic (+) sense RNA is used as a template to synthesize a negative (−) sense RNA, which remains base-paired with the (+) sense RNA to form a double-stranded RNA (dsRNA) called replicative form (RF). Subsequently, the (−) sense RNA within the RF acts as a template for the synthesis of nascent (+) sense RNA. As the nascent (+) sense RNA elongates, it displaces

67 the original (+) sense RNA and remains base pairing with the (−) sense RNA template, forming a
68 three-strand RNA complex called replicative intermediate (RI)[4].
69
70 The host innate immune system, acting as the primary defense against invading pathogens, employs a
71 variety of pattern recognition receptors (PRRs) to recognize conserved molecular structures of pathogens,
72 known as pathogen-associated molecular patterns (PAMPs), which are often vital for the pathogen life
73 cycle[7]. Retinoic acid-inducible gene I (RIG-I)-like receptors (RLRs), a family of cytosolic PRRs that
74 recognize RNA structure-based PAMPs, comprise three members: RIG-1, melanoma
75 differentiation-associated protein 5 (MDA5) and laboratory of genetics and physiology 2 (LGP2)[8]. All
76 RLRs contain a central helicase domain and a carboxy-terminal domain (CTD), which collaboratively detect
77 RNA ligands. Unlike LGP2, RIG-I and MDA5 contain two additional N-terminal caspase activation and
78 recruitment domain (CARD), which is responsible for subsequent signal transduction. As the result, RIG-I
79 and MDA5 can directly recognize RNA ligands and transduce the signals, whereas LGP2 lacks CARD and
80 is believed to play a regulatory role in RIG-I and MDA5 sensing[9, 10]. It has been shown that RIG-I and
81 MDA5 recognize RNA ligands with distinct molecular features. RIG-I detects short dsRNA with a
82 5'-triphosphate (5'ppp) end[11-14]. In addition, RIG-I can detect 5'ppp-single stranded RNA (ssRNA) with
83 certain molecular features yet to be determined. For example, the polyU/UC tract within the hepatitis C virus
84 (HCV) 3'UTR has been demonstrated to activate RIG-I[15]. On the contrary, MDA5 detects long
85 dsRNA[16]. When RIG-I or MDA5 binds to RNA ligands, they undergo conformational changes that
86 facilitate their interaction with CARD domain located in the critical adaptor protein mitochondrial antiviral
87 signaling protein (MAVS). This intermolecular CARD-CARD interaction initiates a signaling cascade that
88 activates the transcription factors NF-κB, interferon regulatory factor 3 (IRF3) and IRF7, which in turn
89 triggers the transcription of the proinflammatory cytokines and the expression of type I and III interferons

(IFNs)[10, 17].

Previous studies showed that MAVS deficiency strongly impairs the induction of cytokines and IFNs in response to DENV infection both in *vivo*[18] and *in vitro*[19-21], supporting an important role of the RLR-mediated signaling in innate immune response to DENV infection. However, it remains obscure which RLR member mediates IFN induction in response to DENV infection. It is reported that DENV-induced IFN responses in African green monkey kidney Vero cells or human lung carcinoma A549 cells were abolished by overexpressing a dominant-negative RIG-I[22], and the IFN response was significantly diminished in DENV-infected human brain microvascular endothelial cells following RIG-I knockdown[23], whereas the knockdown of MDA5 in HEK293 cells had no effect[24]. These results indicate an important role of RIG-I rather than MDA5 in mediating IFN response to the DENV infection. However, it was shown that the IFN response in DENV-infected mouse fibroblast cells was only blocked by silencing both RIG-I and MDA5 but not by silencing either of them[19]. In addition, other studies reported that the silencing RIG-I or MDA5 alone could abrogate the IFN response upon DENV infection in human dendritic cells[20, 21]. These results indicate that both RIG-I and MDA5 may be involved in mediating the innate immune response against DENV infection. Furthermore, the molecular identity of PAMPs recognized by RIG-I or MDA5 during DENV infection also requires further investigations. Maxime and colleagues[24] performed protein affinity purification by overexpressing RIG-I in DENV-infected HEK293 cells, and found that RIG-I-bound DENV RNAs are mainly single-stranded (+) sense viral genomic RNAs with 5'ppp. Therefore, they proposed that the RIG-I recognizes certain secondary structures located within the 5'region of the nascent uncapped single-stranded DENV genomic RNA. However, this experiment was performed in cells overexpressing RLRs, and it remains elusive which exact RNA species are being recognized by RLRs under physiological conditions.

113

114 In this study, we found that both RIG-I and MDA5 were involved in the innate sensing of DENV infection,

115 with RIG-I playing a main role. Furthermore, we demonstrated that RIG-I and MDA5 cooperatively

116 recognized a different moiety in the DENV RF double-stranded RNA to activate the innate immune

117 response.

119 ## Results

120

121 **DENV2 infection-induced IFN response is dependent upon both MDA5 and RIG-I, with RIG-I**

122 **playing a predominant role.**

123

124 DENV employs a multitude of strategies to evade the host innate immune responses, which involves

125 multiple viral proteins such as NS2A, NS2B, NS3, NS4A, NS4B, and NS5[25-30], thus we first evaluated

126 the induction of IFN response in different DENV-infected cell lines. We infected HEK293 cells with

127 DENV2 strain 16681 at a multiplicity of infection (MOI) of 1. Type I and III IFNs as well as intracellular

128 DENV2 RNA levels were determined at the indicated time points post-infection by RT-qPCR. DENV2

129 infection elicited modest interferon response at 24 hours post-infection, but the IFN production dramatically

130 increased at 48 hours post-infection (Fig. 1A-1B). The increased IFN response was found to correlate with

131 the replication of DENV2 RNA (Fig. 1C). Similar to HEK293 cells, DENV2 infection induced robust IFN

132 response in Huh7 and Vero cells (Fig. S1). These results suggested that despite DENV is able to antagonize

133 the host innate immunity to a certain degree, it still triggers strong IFN response in a variety of cells.

134

135 To evaluate the role of MDA5 or RIG-I in innate immune sensing of DENV infection, we generated MDA5

136 or RIG-I knockout HEK293 cells using the CRISPR-Cas9 technology[31]. The loss of MDA5 or RIG-I

137 expression in the knockout cells were verified by the Western blot (Fig. S2A). Next, we transfected these

138 knockout cells with long poly(I:C) or HCV 3'UTR RNA, which are known to be recognized by MDA5 or

139 RIG-I, respectively[15, 16, 32, 33]. As expected, poly(I:C)-induced IFN response was decreased in the

140 MDA5 knockout cells but not in the RIG-I knockout cells, whereas HCV 3'UTR RNA-induced IFN

141 response was impaired only in the RIG-I knockout cells (Fig. S2B-2C). Subsequently, the MDA5 and RIG-I

142 knockout HEK293 cells were infected with DENV2 at a MOI of 1 and the IFN production were determined
143 at 48 hours post-infection by RT-qPCR. The knockout of MDA5 had no apparent effect on interferon
144 production, but the knockout of RIG-I significantly impaired the induction of IFNB1 and IFNL1 (Fig.
145 S2D-2E), despite that viral RNA replication was comparable in the three groups of cells (Fig. S2F). These
146 results suggested RIG-I was the main innate sensor for DENV2 in HEK293 cells.
147
148 Although the knockout of RIG-I dramatically impaired the IFN response induced by DENV2 infection,
149 considerable IFN signaling was still activated in the RIG-I knockout cells (Fig. S2D-2E). We speculated that
150 MDA5 may also contribute to DENV2 infection-triggered IFN signaling albeit to much less extent than
151 RIG-I. As the result, the MDA5 single knockout does not lead to a significant decrease in IFN production,
152 and the contribution of MDA5-mediated signaling may become more pronounced in the RIG-I deficient
153 cells. To test our hypothesis, we knocked out MDA5 in the RIG-I knockout HEK293 cells to generate
154 double knockout (DKO) cells (Fig. S2G). Next we transfected poly(I:C) or HCV 3'UTR RNA into the
155 RIG-I knockout or DKO cells. The result showed that poly(I:C)-induced IFN response was significantly
156 decreased in the DKO cells, while residual HCV 3'UTR RNA-induced IFN response likely resulted from
157 incomplete RIG-I knockout remained unchanged in the DKO cells (Fig. S2H-2I). Next, the MDA5 or RIG-I
158 single knockout and DKO cells were infected with DENV2, and the IFN responses were detected at 48
159 hours post-infection. Interestingly, the IFN signaling was further reduced in the DKO cells compared to the
160 RIG-I single knockout cells (Fig. 1D-1E), whereas the viral replication levels were comparable in all four
161 group of cells (Fig. 1F). These results suggested DENV2 infection-induced IFN response was dependent
162 upon both MDA5 and RIG-I, with RIG-I playing a predominant role.
163
164 **RIG-I and MDA5 recognize the different moiety of DENV2 replicative-form dsRNA.**

165

166 To identify the nature of PAMPs recognized by RIG-I and MDA5 during DENV2 infection, we sought to
167 purify the DENV PAMPs from total RNAs in the DENV2-infected cells through biochemical approaches
168 which have been used for research on Picornavirus[34], influenza A virus and Sendai virus[35]. First,
169 DENV2-infected cellular RNA was extracted from HEK293, Huh7 and Vero cells, and was transfected into
170 HEK293 cells. All of the DENV2-infected cellular RNA induced strong IFN response, whereas the
171 uninfected cellular RNA elicited no IFN production (Fig. 2A-2B). The RNAs extracted from
172 DENV-infected Huh7 cells seemed to possess the most potent ability to trigger IFN response, therefore, we
173 chose DENV2-infected Huh7 cellular RNA in subsequent purification experiments. Next, we assessed
174 whether DENV2-infected cellular RNA-activated IFN response recapitulates the RLR dependency of
175 DENV2 infection-induced IFN response. We transfected the DENV2-infected Huh7 cellular RNA into the
176 MDA5 or RIG-I single knockout, as well as DKO cells. Consistent with the DENV2 infection, the IFN
177 response was not decreased in the MDA5 single knockout cells, but was greatly reduced in the RIG-I single
178 knockout cells, and was further reduced in the DKO cells (Fig. 2C-2D), despite that transfected DENV2
179 RNA levels were comparable in the four groups (Fig. 2E). These results suggested DENV2-infected cellular
180 RNA indeed contained DENV2 PAMPs recognized by RIG-I and MDA5.

181

182 There are four serotypes of DENV (DENV1 to 4)[36]. Next, we assessed the IFN activation in the cells
183 infected by other serotypes of DENV. Huh7 cells were infected with DENV1 strain 16007 and DENV4
184 strain 1036. As shown in Fig. S3A-D, DENV1 and DENV4 infection induced strong interferon responses on
185 day 2 post-infection. We also infected Huh7 cells with DENV3 strain 16562. Consistent with previous
186 studies [37], the replication efficiency of DENV3 was much lower than that of DENV2, and DENV3
187 infection induced modest IFN responses until day 6 post-infection. Next, the total cellular RNAs from

188 DENV1-, DENV3- and DENV4-infected cells were extracted and subsequently transfected into the MDA5
189 and RIG-I single knockout, as well as DKO cells. Consistent with the DENV2, DENV1-, DENV3- and
190 DENV4-infected cellular RNA-induced IFN response required both RIG-I and MDA5, with RIG-I playing a
191 primary role (Fig. S4).
192
193 To analyze the exact RNA species recognized by MDA5 and RIG-I, we purified PAMPs from the
194 DENV2-infected cellular RNA. First, we separated RNAs according to their sedimentation coefficients via a
195 10%-40% sucrose density gradient ultracentrifugation (Fig. S5A). The RNA in each fraction was analyzed
196 by agarose gel electrophoresis. The 5S, 18S and 28S ribosomal RNA were distributed in different fractions
197 (Fig. S5B), and DENV2 RNA was primarily distributed in fractions 7-12 (Fig. S5C). To determine which
198 fraction harbored PAMPs, we transfected RNA in each of these 12 fractions into HEK293 cells and
199 analyzed the IFN response. We found that the RNA in fraction number 7, named DENV2-F7, induced the
200 strongest IFN response (Fig. 3A-3B).
201
202 Next, to further purify PAMPs in DENV2-F7, we separated single stranded RNA (ssRNA) and dsRNA by
203 LiCl differential precipitation (Fig. S6A). The quantification of DENV2 RNA result showed that more viral
204 RNA in fraction 7 was found in the dsRNA fraction than the ssRNA fraction (Fig. S6B), whereas majority
205 of viral RNA in fraction 12 was distributed in the ssRNA fraction (Fig. S6C). Then we transfected
206 DENV2-F7 ssRNA and dsRNA into HEK293 cells and analyzed the IFN response. The results showed that
207 dsRNA (DENV2-F7-dsRNA) triggered stronger IFN response than the ssRNA fraction (DENV2-F7-ssRNA)
208 (Fig. 3C-3D). To assess the RLR dependency, we transfected DENV2-F7-dsRNA into MDA5 or RIG-I
209 single knockout, as well as DKO HEK293 cells. Consistent with DENV2-infected cellular RNA,
210 DENV2-F7-dsRNA was capable of eliciting IFN response through both RIG-I- and MDA5-dependent

211 pathways, with RIG-I playing a main role (Fig. 3E-3F), suggesting that purified DENV2-F7-dsRNA likely
212 represents DENV2 PAMPs in the DENV2-infected cells.
213
214 Next, we performed a strand-specific RNA sequencing analysis on DENV2-F7-dsRNA. Approximately 42%
215 of reads were mapped to DENV2 genomes, and the DENV RNA was greatly enriched in the preparation of
216 DENV2-F7-dsRNA (Fig. S7), suggesting that the DENV PAMPs are likely derived from viral RNA rather
217 than host RNA. DENV sequencing reads were mapped to their positions on the viral genomes. In
218 DENV2-infected cellular RNA, the RNA reads mapping to the (+) sense strand were significantly greater
219 than those mapping to the (-) sense strand (Fig.4A), consistent with a previous finding that positive RNA
220 viruses tend to produce more (+) sense-strand RNA than (-) sense-strand RNA[38]. However, in
221 DENV2-F7-dsRNA, the RNA reads mapping to the both strands were approximately equal across the
222 genome (Fig. 4B). We calculated the ratio of reads mapped to the (+) sense versus those mapped to the (-)
223 sense RNA at each position, expressing this ratio on the log10 scale (Fig. 4C). For DENV2-infected cellular
224 RNA, the average ratio was around 45. However, for DENV2-F7-dsRNA, the ratios were close to 1. The
225 significant differences in read depth mapped to the (+) and (-) sense RNA observed at the ends of genomes
226 might be attributed to a technical bias in sequencing the terminal regions of genes.
227
228 Rapid cooling after high-temperature heating can resolve the duplex of a dsRNA. To further validate the
229 dsRNA feature of DENV2 PAMPs, we heated DENV2-F7-dsRNA at 95℃ for 5 min and rapidly cooled it to
230 0℃, then transfected them into HEK293 cells. The single-stranded HCV 3'UTR RNA was included as a
231 control in this experiment. As shown in Fig. 4D-E, heat-denaturing treatment abolished the capacity of
232 DENV2-F7-dsRNA to elicit IFN response, but had little effect on the HCV 3'UTR RNA-induced IFN
233 response. Altogether, these results suggested that the DENV PAMPs was likely derived from the viral

234 replicative-form (RF) double-stranded RNA.

235

236 The 5'ppp modification of RNA is essential for recognition by RIG-I. Therefore, next we investigated
237 whether DENV2 PAMPs-induced IFN response requires 5'ppp. DENV2-F7-dsRNA was treated with a
238 5'-polyphosphatase (PPase) to remove the γ - and β - phosphates and then transfected into HEK293 cells.
239 After treatment of PPase, DENV2-F7-dsRNA-induced IFN production was greatly reduced (Fig. 5A-5B),
240 while the transfected DENV2-F7-dsRNA levels in the cells remained comparable before and after treatment
241 with PPase (Fig. 5C). These results indicated that DENV2 PAMPs triggered-IFN production required 5'ppp
242 modification. We observed that PPase-treated DENV2-F7-dsRNA still retained considerable capacity to
243 induce IFN production (Fig. 5A-5B). It has been shown that recognition of dsRNA by MDA5 is independent
244 on the 5'ppp of dsRNA[39]. Therefore, we speculated that PPase-treated DENV2-F7-dsRNA might induce
245 the IFN response exclusively through MDA5. To test our hypothesis, we transfected DENV2-F7-dsRNA
246 with or without PPase treatment into MDA5 or RIG-I single knockout HEK293 cells. Consistent with
247 previous results (Fig. 3E), DENV2-F7-dsRNA-induced IFN response was primarily dependent on RIG-I.
248 However, the PPase treatment converted this IFN induction into a MDA5-dependent manner (Fig. 5D-5F).
249 Altogether, these results suggested that recognition of DENV PAMPs by RIG-I is dependent on both
250 double-stranded RNA structure and 5'ppp, while recognition of DENV PAMPs by MDA5 only requires
251 double-stranded RNA structure.

252

253 The mature DENV genomic (+) sense RNA is capped, a process that relies on the presence of stem loop A
254 (SLA) within the 5'UTR. DENV (-) sense RNA, which lacks SLA, remains uncapped[40]. However, it
255 remains uncertain whether the (+) sense RNA within the RF is capped. In West Nile virus (WNV)-infected
256 cells, the cap is shown to be present only on the genomic (+) sense RNA but not on the RF[41]. To explore

257 whether the 5' ends of the DENV RF (+) and (-) sense RNA were modified with 5'ppp, we treated
258 DENV2-F7-dsRNA with PPase to remove the γ - and β - phosphates and then digested the RNA with
259 5'–3' exonuclease Xrn1, which digests RNA with a 5'monophosphate (5'p). After treatment with PPase and
260 Xrn1, we assessed the RNA degradation by RT-qPCR using a primer set targeting the 5' region of the
261 DENV2 (+) stand and (-) strand respectively (Fig. S8A). As controls for the assay, we also included *in vitro*
262 transcribed (IVT) replicon (+) sense ssRNA bearing a 5'ppp and uninfected Huh7 cellular RNAs containing
263 5' capped ACTB mRNA. As expected, the PPase treatment rendered the IVT DENV2 replicon ssRNA but
264 not capped ACTB mRNA susceptible to digestion by Xrn1 (Fig. S8B-8C). Importantly, the PPase treatment
265 rendered both (+) and (-) strands of DENV2-F7-dsRNA susceptible to digestion by Xrn1 (Fig. 5G-5H),
266 suggesting that the both strands of DENV2 RF contained a 5'ppp. To further assess whether the 5'end of (+)
267 sense RNA was capped with m7GpppAm. We treated DENV2-F7-dsRNA with mRNA decapping enzyme
268 (MDE) to remove the cap-0 or cap-1 structure, producing a 5'p end, and then digested the RNA with Xrn1
269 (Fig. S8D). The uninfected Huh7 cellular RNAs containing ACTB mRNA with a 5' cap and BCYRN1 RNA
270 with a 5'ppp[42] were included as controls for the assay. As expected, the MDE treatment rendered the
271 capped ACTB mRNA but not BCYRN1 RNA susceptible to digestion by Xrn1 (Fig. S8E-8F). Both (+) and
272 (-) strands of DENV2-F7-dsRNA remained stable upon the MDE-Xrn1treatment (Fig. 5I-5J), suggesting
273 that neither strand of DENV2 RF was capped. Taken together, our results demonstrated that (+) and (-)
274 sense RNA of the DENV2 PAMP dsRNA, similar to WNV RF[41], contained a 5'ppp.
275
276 ***In vitro* reconstituted DENV RF dsRNA recapitulates the features of DENV PAMPs**
277
278 Next, we sought to confirm the nature of DENV PAMPs by reconstituting DENV RF *in vitro*. The (+) and (-)
279 sense DENV2 replicon RNAs bearing a 5'ppp were synthesized by *in vitro* transcription, and then annealed

280 at a ratio of 1:1 to generate a dsRNA mimicking DENV RF, which was confirmed by size-exclusion
281 chromatography (Fig. S9). Next, we investigated whether the reconstituted DENV RF dsRNA displays the
282 similar features of DENV2-F7-dsRNA. We transfected the reconstituted DENV RF dsRNA into MDA5 or
283 RIG-I single knockout, as well as DKO HEK293 cells. As expected, the reconstituted DENV RF
284 induced-IFN response required both MDA5 and RIG-I, with RIG-I playing a predominant role (Fig. 6A-6B).
285 Subsequently, the reconstituted DENV RF dsRNA was treated with PPase to generate 5'p, and then
286 transfected into MDA5 or RIG-I single knockout HEK293 cells. Consistent with DENV2-F7-dsRNA, the
287 treatment with PPase reduced the capacity of the reconstituted DENV RF to induce IFN response and
288 converted the IFN production from a RIG-I-dependent to a MDA5-dependent manner (Fig. 6C-6E). Taken
289 together, these results demonstrated that the reconstituted DENV RF dsRNA exhibited similar
290 characteristics to the purified DENV PAMP.

292 **Discussion**

293

294 Currently, it remains unclear which PRR exactly mediates IFN production during DENV infection, in
295 particular, the importance of RIG-I versus MDA5 in sensing DENV PAMP remains a debatable subject.
296 Additionally, the exact molecular identity of DENV PAMPs recognized by RLRs under physiological
297 conditions has not yet been fully explored. In this study, we uncovered a cooperative contribution of RIG-I
298 and MDA5 in innate immune sensing DENV infection, with RIG-I playing a predominant role. Next, we
299 purified PAMP RNA from DENV-infected cells using sucrose density gradient centrifugation and LiCl
300 differential precipitation. Using strand-specific RNA-seq, heat denaturing, 5' end RNA
301 modification-specific enzymatic digestions as well as *in vitro* reconstitution, we demonstrated that the
302 DENV PAMP is likely a DENV RF dsRNA bearing 5'ppp modifications at the both strands.

303

304 RLRs recognize dsRNA-like structures to activate the IFN response during RNA virus infection. However,
305 the exact nature of these dsRNA-like structures generated during RNA virus infection remains an important
306 subject to explore for many RNA viruses. A number of studies explored RLRs-associated RNAs by
307 precipitating overexpressed or endogenous RLRs, followed by next-generation sequencing[24, 35, 43-47].
308 However, this approach is critically dependent on the efficiency and specificity of the RNA precipitation
309 process. In addition, RLRs-bound RNAs may have undergone irreversible conformational changes upon the
310 RLR binding that lead to loss of the immunostimulatory capability when these RNAs are
311 immunoprecipitated and re-introduced into a cell. In our study, we purified PAMPs from the virus-infected
312 cells by employing sucrose density gradient centrifugation and LiCl differential precipitation. This approach
313 results in a high recovery rate of PAMPs and ensures the stability of PAMPs throughout the purification
314 procedure. Therefore, our method can also be applied to study the identity of PAMPs of other RNA viruses

315 in the context of their infection.

316

317 We found that single RIG-I knockout led to a significant decrease in IFN production during DENV infection,
318 whereas single MDA5 knockout had no effect. However, the function of MDA5 became more pronounced
319 in the RIG-I deficient cells (Fig. 1D-1F and Fig. S4). Maxime and colleagues[24] showed that RIG-I is the
320 main RLR sensor of DENV2 and DENV4 infections in HEK293 cells, whereas diminished expression of
321 MDA5 had little or no effect on IFN production. In HEK293 cells, the contribution of MDA5 to the
322 initiation of the IFN response during DENV infection is indeed quite modest and could be overlooked. Joris
323 K and colleagues[20, 21] reported that silencing RIG-I, MDA5 alone or together strongly abrogated the
324 IFNs and cytokines expression upon DENV2 infection in human dendritic cells. Our work suggested that
325 RIG-I and MDA5 may act simultaneously to sense DENV RF dsRNA despite that these two PRRs tend to
326 recognize a dsRNA with different molecular features. The RF bearing 5'ppp may exist during replication of
327 other positive-stranded RNA viruses, for example HCV[42] and WNV[41]. Hence, the cooperative detection
328 of PAMP by RIG-I and MDA5 is likely a more general phenomenon during RNA virus infections. The
329 relative contributions of RIG-I versus MDA5 to the IFN response in the context of these RNA virus
330 infections may vary across different cell types, likely due to the disparities in the relative strength of the
331 RIG-I and MDA5 signaling pathways as well as the availability of corresponding PAMPs in these cells. For
332 example, Feng and colleagues [34] reported that MDA5 but not RIG-I detected dsRNA RF during
333 Picornavirus infection. This may be due to the fact that the (+) sense and (-) sense strands of Picornaviral RF
334 dsRNA are covalently linked with VPg , a small peptide of 20–24 amino acids that serves as a primer for
335 RNA synthesis[48], thereby preventing them being recognized by RIG-I. Consequently, the Picornavirus RF
336 lacking 5'ppp exclusively activates MDA5 but not RIG-I.

337

338 Maxime and colleagues[24] proposed that RIG-I detected 5'ppp nascent (+) sense RNA of the DENV RI
339 during viral infection. It is reported that DENV RI sediments between 20 and 28S, and insoluble in 2 M
340 LiCl[38]. According to these characteristics, DENV RI is likely to be distributed in F7 to F9 in our sucrose
341 density gradient centrifugation, and enriched in a ssRNA preparation by LiCl differential precipitation.
342 However, compared to F7 and F7-dsRNA samples, F8, F9 and F7-ssRNA samples induce much less IFN
343 response (Fig. 3). In addition, Nicolas and colleagues[46] reported that RIG-I detected RNA polymerase III
344 (Pol3)-transcribed Y RNA and vault RNA (vtRNA) during DENV4 infection. However, our results showed
345 that viral RNAs were significantly enriched in the DENV2-F7-dsRNA preparation, strongly supporting that
346 DENV PAMPs are likely viral RNAs instead of host cellular RNAs. Taken together, although our results do
347 not completely rule out a minor role of DENV RI, Y RNA and vtRNA in activating IFN response during
348 DENV infection, the major DENV PAMPs are derived from DENV RF dsRNA.
349
350 It is well known that DENV (+) sense RNA is capped, but it remains to be elucidated at which point during
351 its synthesis this capping reaction occurs. Valerie J and colleagues proposed two models: co-transcriptional
352 model and post-transcriptional model[4]. In the co-transcriptional model, as the nascent (+) sense RNA is
353 transcribed from the DENV RF, the RNA is capped. Following the synthesis of a short stretch of the (+)
354 sense RNA, the 5' end of this newly synthesized RNA is capped by NS3 and NS5 proteins. Subsequently,
355 the 5'capped (+) sense RNA is extended until the entire strand is fully replicated. Ultimately, a dsRNA
356 containing a capped (+) sense and a free capped (+) sense RNA are produced. In post-transcriptional model,
357 capping takes place on the pre-existing full-length (+) sense but not nascent (+) sense RNA. After the
358 double-stranded RF is unwound by the NS3 helicase, the (+) sense RNA is capped. In the end, a new
359 dsRNA and a free capped (+) sense RNA are synthesized. The primary distinction between the two models
360 is whether the (+) sense RNA within the RF is capped. In our study, we found that both (+) and (-) sense

361 RNA of RF were modified with 5'ppp, and this result provided an important piece of evidence to support the
362 post-transcriptional model.
363
364 DENV infection has the potential to induce viral hemorrhagic fever, which is characterized by increased
365 vascular permeability, hemorrhage and shock. Anon and colleagues proposed[49] that severe dengue is
366 mediated by multiple immune effectors. As of now, there are no specific antiviral agents for dengue,
367 treatment relies on fluid replacement and the administration of analgesics to alleviate symptoms. Our study
368 identified RIG-I and MDA5 cooperatively detected the DENV RF during viral infection, providing a
369 potential therapeutic target for the treatment DENV hemorrhagic fever.

371 **Materials and methods**

372

373 **Cell culture and virus preparation**

374 HEK293, Huh7, Vero cells were purchased from the National Collection of Authenticated Cell Cultures
375 (Shanghai, China). These cells and their derivatives were maintained in complete Dulbecco's modified
376 Eagle's medium (DMEM) (Invitrogen, Carlsbad, CA, USA) supplemented with 10% fetal bovine serum, 10
377 mM HEPES, 2 mM L-glutamine, 100 U of penicillin/ml, and 100 mg of streptomycin/ml. All cells were
378 cultured in humidified air containing 5% CO_2 at 37℃. DENV1/2/3/4 viruses were obtained from Dr. Xia Jin
379 (Institut Pasteur of Shanghai, Chinese Academy of Sciences). All DENV viruses were propagated in Vero
380 cells and titrated by immunofluorescence assay.

381

382 **Reagents**

383 Long poly(I:C) was purchased from Invivogen (San Diego, CA). Preparation of HCV 3'UTR RNA was as
384 previously described[17]. 5' polyphosphatase was purchased from Epicentre (RP8092). The mRNA
385 decapping enzyme was purchased from New England Biolabs (M0608S). Xrn1 was purchased from New
386 England Biolabs (M0338S).

387

388 **Generation of RIG-I- and MDA5-knockout HEK293 cells by lenti-CRISPR-Cas9**

389 The sequence of sgRNA targeting RIG-I was: 5'-GGCCATGTAGCTCAGGATGT-3'; sgRNA targeting
390 MDA5 was 5'-CGAATTCCCGAGTCCAACCA-3'; sgRNA targeting control was 5'-
391 AACCGCATCGAGCTGA-3'. HEK293T cells were seeded into six-well plates 1 day before transfection
392 and then cotransfected with 1.5 μg of psPAX2 plasmid, 1 μg of pMD2.G plasmid, and 2 μg of
393 lenti-Cas9-sgRNAs using polyethylenimine (Polysciences). Culture supernatants containing lentiviruses

394 were harvested at 48 hours post-transfection, passed through a 0.45-μm-pore-size filter, and used to infect
395 HEK293 cells. Transduced cells were selected in medium containing 1 μg/mL of puromycin for 2 days. To
396 generate DKO cells, RIG-I knockout HEK293 cells were infected with lentiviruses expressing sgMDA5
397 harboring blasticidin resistance gene. As control, sgControl, sgRIG-I and sgMDA5 cells were infected with
398 lentiviruses expressing sgControl harboring blasticidin resistance gene. Transduced cells were selected in
399 medium containing 15 μg/mL of blasticidin for 2 days. The knockout efficiency was verified by Western
400 blot.
401
402 **RNA isolation and quantitative RT-PCR (RT-qPCR)**
403 The protocol was as described previously[50]. In brief , total cellular RNA was isolated using TRNzol
404 reagent (Tiangen, Beijing, China). RNA heated at 95°C for 5 minutes and immediately placed on ice to cool
405 down to 0°C, followed by RT-qPCR. RT-qPCR was carried out utilizing SYBR green real-time PCR master
406 mix (Toyobo). The sequences of the qPCR primers for GAPDH and IFNL1 were described previously[51].
407 Other qPCR primers were as follows: IFNB1-F, 5'- GTCACTGTGCCTGGACCATAG-3'; IFNB1-R,
408 5'-GTTTCGGAGGTAACCTGTAAGTC-3'.
409 DENV2 RNA-F, 5'-AGTAGTTAGTCTACGTGGAC-3'; DENV2 RNA-R, 5'-
410 GTTGACACGCGGTTTCTCTC-3'. DENV1 RNA-F, 5'-AGTTGTTAGTCTACGTGGAC-3'; DENV1
411 RNA-R, 5'-GTTGACACGCGGTTTCTCGC-3'. DENV3 RNA-F, 5'-AGTTGTTAGTCTACGTGGAC-3';
412 DENV3 RNA-R, 5'- GTTGACACACGGTTTCTCAC-3'. DENV4 RNA-F,
413 5'-AGTTGTTAGTCTGTGTGGAC-3'; DENV4 RNA-R, 5'-GTTGATACGCGGTTTCTCTC-3'. qPCR
414 primers for GAPDH used in Fig. S1 (target both human and green monkey) were as follows: GAPDH-F,
415 5'-GCTGAGTACGTCGTGGAGTC-3'; GAPDH-R, 5'-TGATGACCCTTTTGGCTCCC-3'.
416 The qPCR primers used in 5' end RNA modification-specific enzymatic digestions (Fig. S8 and Fig.5) were

417 as follows: ACTB-F, 5’-GCCTCGCCTTTGCCGA-3’; ACTB-R, 5’-AGGAATCCTTCTGACCCATGC-3’.
418 BCYRN1-F, 5’-GAGGATAGCTTGAGCCCAGG-3’; BCYRN1-R, 5’-
419 GCTTTGAGGGAAGTTACGCTTAT-3’. The qPCR primers for 5'end of DENV2 (+) sense RNA were
420 same as primers for DENV2 RNA as mentioned above. The qPCR primers for 5'end of DENV2 (-) sense
421 RNA: F, 5’-TTGAGTAAACTGTGCAGCCTGTAGCTC-3’; R,
422 5’-GAGACAGCAGGATCTCTGGTCTTTC-3’.
423 The qPCR primers used for detecting DENV2 RNA level following sucrose density gradient centrifugation
424 (Fig. S5A) and LiCl differential precipitation (Fig. S6B-6C) were designed to target DENV2 NS3-coding
425 region as follow: DENV2 NS3-F, 5’-AGCATCGAAGACAACCCAGA-3’; DENV2 NS3-R,
426 5’-CAACTCTAGTGGGGGCCAAG-3’. For the absolute quantification assay (Fig. S7), DENV2 RNA
427 levels in DENV2-infected cellular RNA, DENV2-F7 and DENV2-F7-dsRNA samples were determined
428 relative to a standard curve comprised of serial dilutions of DENV2 replicon plasmid. The qPCR primers
429 were designed to target DENV2 NS3-coding region as mentioned above.
430
431 **RNA transfection**
432 One day before transfection, 1×10^5 HEK293 cells were seeded onto 48-well plates and RNA was
433 transfected using X-TremeGENE HP DNA Transfection Reagent (Roche, Basel, Switzerland) following the
434 manufacturer’s instructions.
435
436 **Western blotting**
437 The protocol was as described previously[51]. The antibody recognizing MDA5, RIG-I, were obtained from
438 Cell Signaling Technology (Danvers, MA, USA). Antibody against ACTB was obtained from Abmart
439 (Shanghai, China).

440

441 **Sucrose density gradient centrifugation**

442 Huh7 cells were infected with DENV2 at MOI of 1. The cells were collected at 48 hpi. Total cellular RNA
443 was extracted using TRNzol reagent. 800 μg (200 μl) DENV2-infected Huh7 cellular RNA were separated
444 by centrifugation in 10%–40% (w/w) sucrose gradient (buffer 20 mM Na-acetate, 100 mM NaCl, 1 mM
445 EDTA, 10U/ml RNasin) at 140,000 ×g in an SW60 Ti rotor (Beckman) at 4°C for 16 h. 12 fractions were
446 collected from top to bottom with 330 μl in each fraction. RNA of 12 fractions were precipitated with
447 isopropanol and then diluted in 200 μl DEPC H_2O.

448

449 **LiCl differential precipitation**

450 RNA was added with LiCl to a final concentration of 2 M, incubated at 4°C for 16 h. The ssRNA fraction
451 was precipitated by centrifugation at 16,000 ×g for 30 min at 4°C. The supernatant was subjected to
452 ethanol precipitate in the presence of 0.8M LiCl to precipitate the dsRNA fraction. RNA pellets were
453 washed with 75% ethanol, air-dried, and dissolved in DEPC H_2O.

454

455 **Strand-specific RNA-seq and data analysis**

456 The cDNA library construction and sequencing were conducted by NeoBio, Shanghai, China.
457 DENV2-infected cellular RNA and DENV2-F7-dsRNA were used as the starting material. To analyze all
458 RNA species present, the poly(A) RNA isolation step was omitted. The Ribo-Zero rRNA Removal Kit
459 (Epicentre, USA) was used for DENV2-infected cellular RNA to remove rRNA. The DENV2-F7-dsRNA
460 had a low rRNA content, therefore, the step of removing rRNA was omitted. The Truseq Stranded mRNA
461 sample preparation kit (Illumina,USA) was used for the RNA fragmentation, the first-strand cDNA
462 synthesis, and the second-strand cDNA synthesis. The double strands cDNA was then purified for end repair,

463 dA tailing, adaptors ligation and DNA fragments enrichment. Quantify the libraries using Qubit
464 (invitrogen,CA,USA) according to the Qubit user Guide. The libraries were then pooled and sequenced on
465 NovaSeq 6000 (Illumina). The raw data was handled by fastp (version 0.23.2) and data quality was checked
466 by FastQC (version 0.12.1). Clean reads were aligned to the genome files build with the human genome
467 (hg38) plus DENV2 strain 16681 sequence, and the alignment was performed by bwa (Version 0.7.17).
468 Samtools (version 1.15.1) was used to extract reads that match the forward and reverse chains, and saved as
469 two new bam files respectively. Finally, featureCounts (v2.0.3) was used to perform the quantification of
470 genes using the above bam files.
471
472 **5'-end RNA modification-specific enzymatic digestion assays**
473 For samples with lower RNA quantity, such as (IVT) DENV2 replicon (+) sense RNA and
474 DENV-F7-dsRNA were supplemented with 10 μg uninfected Huh7 cellular RNA when treated with PPase
475 or MDE. To convert 5'ppp to 5'p, 0.5 U/μl of PPase in 40 μl of 1× reaction buffer (provided by the kit) for
476 30 min at 37°C followed by purification with TRNzol reagent. To convert 5'cap to 5'p, 5 U/μl of MDE in 20
477 μl of 1× reaction buffer (provided by the kit) for 60 min at 37°C followed by purification with TRNzol
478 reagent. PPase or MDE treated DENV-F7-dsRNA was denatured by heat (95 °C for 5 min) to generate
479 ssRNA for Xrn1 degradation. For 5'p RNA degradation, RNA was treated with 0.1 U/μl of Xrn1 in 10 μl of
480 1× NEB buffer 3 for 60 min at 37 °C followed by purification with TRNzol reagent. The RNA degradation
481 efficiency was determined by RT-qPCR.
482
483 ***In vitro* reconstitution of DENV2 RF dsRNA**
484 PCR products were used as DNA templates for *in vitro* transcription. The DNA templates were amplified
485 from DENV2 replicon plasmid[52]. To amplify DNA templates for DENV2 replicon (+) sense RNA using

486 the following primers, F, 5'-GCCGCAAATTTAATACGACTCACTATAGAGT-3', and R, 5'-
487 GGTGCTGTTGAATCAACAGGTTCT-3'. To amplify DNA templates for DENV2 replicon (-) sense RNA
488 using the following primers, F, 5'-AGTTGTTAGTCTACGTGGACCGACAAAGACAGATTCT-3', and R,
489 5'-GCCGCAAATTTAATACGACTCACTATAGAGAACCTGTTGATTCAACAGCACCATTCCATTTT
490 CT-3'. *In vitro* transcription of DENV2 replicon (+) and (-) sense RNA were performed using a
491 MEGAscript T7 transcription kit (Invitrogen, Carlsbad, CA, USA) following the manufacturer's protocol.
492 To form a double-stranded substrate, the DENV2 replicon (+) and (-) sense RNA were mixed in equimolar
493 concentrations in 20 mM Tris buffer (pH 8.0) containing 1 mM EDTA and 0.1 M NaCl. The mixture was
494 heated at 95°C for 5 min and then cooled to 30°C for 40 min. The annealed duplex was extracted by TRNzol
495 reagent.
496
497 **Size-exclusion chromatography (SEC)**
498 The SEC was performed with a Bio SEC-5 2000 Å (i.d. 7.8 mm; length 300 mm) column (Agilent
499 Technologies, Foster City, CA), with 100 mM ammonium acetate (pH 7.0) as the mobile phase. Isocratic
500 separations were performed at 0.5 ml/min with RNA elution monitored by UV absorbance on the Agilent
501 1200 HPLC system.
502
503 **Statistical analysis**
504 GraphPad Prism 8 software (GraphPad Software Inc.) was used for statistical analysis. Statistical analyses
505 were performed using unpaired, two-tailed Student's t test. P values <0.05 was considered statistically
506 significant.

Acknowledgements

We thank Dr. Xia Jin (Institut Pasteur of Shanghai, Chinese Academy of Sciences) for providing DENV1, DENV2, DENV3 and DENV4. We thank Dr. Gong Cheng (Tsinghua University, China) for providing the DENV2 replicon plasmid. We thank Yujiao Qin (Shanghai Institute of Immunity and Infection, Chinese Academy of Sciences) for providing technical support on size-exclusion chromatography. This work was supported by the grants from Key Research and Development Program, Ministry of Science and Technology of China (2021YFC2300204, 2022YFC2303300), National Natural Science Foundation of China (32070944, 32261143735), Program of Shanghai Academic/Technology Research Leader (22XD1403800) to J.Z.

Author Contributions: S.Y. designed and conducted investigation, analyzed the data, and prepared the manuscript. Y.L., Y.C. and B.L. assisted the investigation. J.Z. conceived the idea, designed investigation, supervised the study and edited the manuscript.

Declaration of interests: We declare no conflict of interest.

Data Availability: All data are available in the main text or the supplementary materials.

526 **References**

527 1. Holmes EC, Twiddy SS. The origin, emergence and evolutionary genetics of dengue virus. Infection, genetics and evolution :
528 journal of molecular epidemiology and evolutionary genetics in infectious diseases. 2003;3(1):19-28. Epub 2003/06/12. doi:
529 10.1016/s1567-1348(03)00004-2. PubMed PMID: 12797969.
530 2. Islam MT, Quispe C, Herrera-Bravo J, Sarkar C, Sharma R, Garg N, et al. Production, Transmission, Pathogenesis, and Control
531 of Dengue Virus: A Literature-Based Undivided Perspective. BioMed research international. 2021;2021:4224816. Epub
532 2021/12/28. doi: 10.1155/2021/4224816. PubMed PMID: 34957305; PubMed Central PMCID: PMCPMC8694986.
533 3. Shang W, Liu J, Yang J, Hu Z, Rao X. Dengue virus-like particles: construction and application. Applied microbiology and
534 biotechnology. 2012;94(1):39-46. Epub 2012/03/03. doi: 10.1007/s00253-012-3958-7. PubMed PMID: 22382168.
535 4. Klema VJ, Padmanabhan R, Choi KH. Flaviviral Replication Complex: Coordination between RNA Synthesis and 5'-RNA
536 Capping. Viruses. 2015;7(8):4640-56. Epub 2015/08/20. doi: 10.3390/v7082837. PubMed PMID: 26287232; PubMed Central
537 PMCID: PMCPMC4576198.
538 5. Fernandez-Garcia MD, Mazzon M, Jacobs M, Amara A. Pathogenesis of flavivirus infections: using and abusing the host cell.
539 Cell host & microbe. 2009;5(4):318-28. Epub 2009/04/22. doi: 10.1016/j.chom.2009.04.001. PubMed PMID: 19380111.
540 6. Guzman MG, Gubler DJ, Izquierdo A, Martinez E, Halstead SB. Dengue infection. Nature reviews Disease primers.
541 2016;2:16055. Epub 2016/08/19. doi: 10.1038/nrdp.2016.55. PubMed PMID: 27534439.
542 7. Akira S, Uematsu S, Takeuchi O. Pathogen recognition and innate immunity. Cell. 2006;124(4):783-801. Epub 2006/02/25.
543 doi: 10.1016/j.cell.2006.02.015. PubMed PMID: 16497588.
544 8. Hartmann G. Nucleic Acid Immunity. Advances in immunology. 2017;133:121-69. Epub 2017/02/22. doi:
545 10.1016/bs.ai.2016.11.001. PubMed PMID: 28215278; PubMed Central PMCID: PMCPMC7112058.
546 9. Hei L, Zhong J. Laboratory of genetics and physiology 2 (LGP2) plays an essential role in hepatitis C virus infection-induced
547 interferon responses. Hepatology (Baltimore, Md). 2017;65(5):1478-91. Epub 2017/01/17. doi: 10.1002/hep.29050. PubMed
548 PMID: 28090671.
549 10. Rehwinkel J, Gack MU. RIG-I-like receptors: their regulation and roles in RNA sensing. Nature reviews Immunology.
550 2020;20(9):537-51. Epub 2020/03/24. doi: 10.1038/s41577-020-0288-3. PubMed PMID: 32203325; PubMed Central PMCID:
551 PMCPMC7094958.
552 11. Hornung V, Ellegast J, Kim S, Brzózka K, Jung A, Kato H, et al. 5'-Triphosphate RNA is the ligand for RIG-I. Science (New York,
553 NY). 2006;314(5801):994-7. Epub 2006/10/14. doi: 10.1126/science.1132505. PubMed PMID: 17038590.
554 12. Pichlmair A, Schulz O, Tan CP, Näslund TI, Liljeström P, Weber F, et al. RIG-I-mediated antiviral responses to single-stranded
555 RNA bearing 5'-phosphates. Science (New York, NY). 2006;314(5801):997-1001. Epub 2006/10/14. doi:
556 10.1126/science.1132998. PubMed PMID: 17038589.
557 13. Schlee M, Roth A, Hornung V, Hagmann CA, Wimmenauer V, Barchet W, et al. Recognition of 5' triphosphate by RIG-I
558 helicase requires short blunt double-stranded RNA as contained in panhandle of negative-strand virus. Immunity.
559 2009;31(1):25-34. Epub 2009/07/07. doi: 10.1016/j.immuni.2009.05.008. PubMed PMID: 19576794; PubMed Central PMCID:
560 PMCPMC2824854.
561 14. Schmidt A, Schwerd T, Hamm W, Hellmuth JC, Cui S, Wenzel M, et al. 5'-triphosphate RNA requires base-paired structures
562 to activate antiviral signaling via RIG-I. Proceedings of the National Academy of Sciences of the United States of America.
563 2009;106(29):12067-72. Epub 2009/07/04. doi: 10.1073/pnas.0900971106. PubMed PMID: 19574455; PubMed Central PMCID:
564 PMCPMC2705279.
565 15. Saito T, Owen DM, Jiang F, Marcotrigiano J, Gale M, Jr. Innate immunity induced by composition-dependent RIG-I
566 recognition of hepatitis C virus RNA. Nature. 2008;454(7203):523-7. Epub 2008/06/13. doi: 10.1038/nature07106. PubMed
567 PMID: 18548002; PubMed Central PMCID: PMCPMC2856441.
568 16. Kato H, Takeuchi O, Mikamo-Satoh E, Hirai R, Kawai T, Matsushita K, et al. Length-dependent recognition of
569 double-stranded ribonucleic acids by retinoic acid-inducible gene-I and melanoma differentiation-associated gene 5. The Journal
570 of experimental medicine. 2008;205(7):1601-10. Epub 2008/07/02. doi: 10.1084/jem.20080091. PubMed PMID: 18591409;
571 PubMed Central PMCID: PMCPMC2442638.

572 17. Ding Q, Huang B, Lu J, Liu YJ, Zhong J. Hepatitis C virus NS3/4A protease blocks IL-28 production. European journal of
573 immunology. 2012;42(9):2374-82. Epub 2012/06/12. doi: 10.1002/eji.201242388. PubMed PMID: 22685015.
574 18. Perry ST, Prestwood TR, Lada SM, Benedict CA, Shresta S. Cardif-mediated signaling controls the initial innate response to
575 dengue virus in vivo. Journal of virology. 2009;83(16):8276-81. Epub 2009/06/06. doi: 10.1128/jvi.00365-09. PubMed PMID:
576 19494017; PubMed Central PMCID: PMCPMC2715757.
577 19. Loo YM, Fornek J, Crochet N, Bajwa G, Perwitasari O, Martinez-Sobrido L, et al. Distinct RIG-I and MDA5 signaling by RNA
578 viruses in innate immunity. Journal of virology. 2008;82(1):335-45. Epub 2007/10/19. doi: 10.1128/jvi.01080-07. PubMed PMID:
579 17942531; PubMed Central PMCID: PMCPMC2224404.
580 20. Sprokholt JK, Kaptein TM, van Hamme JL, Overmars RJ, Gringhuis SI, Geijtenbeek TBH. RIG-I-like Receptor Triggering by
581 Dengue Virus Drives Dendritic Cell Immune Activation and T(H)1 Differentiation. Journal of immunology (Baltimore, Md : 1950).
582 2017;198(12):4764-71. Epub 2017/05/17. doi: 10.4049/jimmunol.1602121. PubMed PMID: 28507028.
583 21. Sprokholt JK, Kaptein TM, van Hamme JL, Overmars RJ, Gringhuis SI, Geijtenbeek TBH. RIG-I-like receptor activation by
584 dengue virus drives follicular T helper cell formation and antibody production. PLoS pathogens. 2017;13(11):e1006738. Epub
585 2017/12/01. doi: 10.1371/journal.ppat.1006738. PubMed PMID: 29186193; PubMed Central PMCID: PMCPMC5724900.
586 22. Chang TH, Liao CL, Lin YL. Flavivirus induces interferon-beta gene expression through a pathway involving RIG-I-dependent
587 IRF-3 and PI3K-dependent NF-kappaB activation. Microbes and infection. 2006;8(1):157-71. Epub 2005/09/27. doi:
588 10.1016/j.micinf.2005.06.014. PubMed PMID: 16182584.
589 23. da Conceição TM, Rust NM, Berbel AC, Martins NB, do Nascimento Santos CA, Da Poian AT, et al. Essential role of RIG-I in
590 the activation of endothelial cells by dengue virus. Virology. 2013;435(2):281-92. Epub 2012/10/24. doi:
591 10.1016/j.virol.2012.09.038. PubMed PMID: 23089253.
592 24. Chazal M, Beauclair G, Gracias S, Najburg V, Simon-Lorière E, Tangy F, et al. RIG-I Recognizes the 5' Region of Dengue and
593 Zika Virus Genomes. Cell reports. 2018;24(2):320-8. Epub 2018/07/12. doi: 10.1016/j.celrep.2018.06.047. PubMed PMID:
594 29996094.
595 25. Castillo Ramirez JA, Urcuqui-Inchima S. Dengue Virus Control of Type I IFN Responses: A History of Manipulation and
596 Control. Journal of interferon & cytokine research : the official journal of the International Society for Interferon and Cytokine
597 Research. 2015;35(6):421-30. Epub 2015/01/30. doi: 10.1089/jir.2014.0129. PubMed PMID: 25629430; PubMed Central PMCID:
598 PMCPMC4490770.
599 26. Coldbeck-Shackley RC, Eyre NS, Beard MR. The Molecular Interactions of ZIKV and DENV with the Type-I IFN Response.
600 Vaccines. 2020;8(3). Epub 2020/09/18. doi: 10.3390/vaccines8030530. PubMed PMID: 32937990; PubMed Central PMCID:
601 PMCPMC7565347.
602 27. Gack MU, Diamond MS. Innate immune escape by Dengue and West Nile viruses. Current opinion in virology.
603 2016;20:119-28. Epub 2016/10/30. doi: 10.1016/j.coviro.2016.09.013. PubMed PMID: 27792906; PubMed Central PMCID:
604 PMCPMC5578430.
605 28. Lee MF, Voon GZ, Lim HX, Chua ML, Poh CL. Innate and adaptive immune evasion by dengue virus. Frontiers in cellular and
606 infection microbiology. 2022;12:1004608. Epub 2022/10/04. doi: 10.3389/fcimb.2022.1004608. PubMed PMID: 36189361;
607 PubMed Central PMCID: PMCPMC9523788.
608 29. Morrison J, Aguirre S, Fernandez-Sesma A. Innate immunity evasion by Dengue virus. Viruses. 2012;4(3):397-413. Epub
609 2012/05/17. doi: 10.3390/v4030397. PubMed PMID: 22590678; PubMed Central PMCID: PMCPMC3347034.
610 30. Uno N, Ross TM. Dengue virus and the host innate immune response. Emerging microbes & infections. 2018;7(1):167. Epub
611 2018/10/12. doi: 10.1038/s41426-018-0168-0. PubMed PMID: 30301880; PubMed Central PMCID: PMCPMC6177401.
612 31. Shalem O, Sanjana NE, Hartenian E, Shi X, Scott DA, Mikkelson T, et al. Genome-scale CRISPR-Cas9 knockout screening in
613 human cells. Science (New York, NY). 2014;343(6166):84-7. Epub 2013/12/18. doi: 10.1126/science.1247005. PubMed PMID:
614 24336571; PubMed Central PMCID: PMCPMC4089965.
615 32. Uzri D, Gehrke L. Nucleotide sequences and modifications that determine RIG-I/RNA binding and signaling activities.
616 Journal of virology. 2009;83(9):4174-84. Epub 2009/02/20. doi: 10.1128/jvi.02449-08. PubMed PMID: 19224987; PubMed
617 Central PMCID: PMCPMC2668486.
618 33. Xu Y, Zhong J. Innate immunity against hepatitis C virus. Current opinion in immunology. 2016;42:98-104. Epub

619 2016/10/30. doi: 10.1016/j.coi.2016.06.009. PubMed PMID: 27366996.
620 34. Feng Q, Hato SV, Langereis MA, Zoll J, Virgen-Slane R, Peisley A, et al. MDA5 detects the double-stranded RNA replicative
621 form in picornavirus-infected cells. Cell reports. 2012;2(5):1187-96. Epub 2012/11/13. doi: 10.1016/j.celrep.2012.10.005.
622 PubMed PMID: 23142662; PubMed Central PMCID: PMCPMC7103987.
623 35. Rehwinkel J, Tan CP, Goubau D, Schulz O, Pichlmair A, Bier K, et al. RIG-I detects viral genomic RNA during negative-strand
624 RNA virus infection. Cell. 2010;140(3):397-408. Epub 2010/02/11. doi: 10.1016/j.cell.2010.01.020. PubMed PMID: 20144762.
625 36. Holmes EC. Molecular epidemiology and evolution of emerging infectious diseases. British medical bulletin.
626 1998;54(3):533-43. Epub 1999/05/18. doi: 10.1093/oxfordjournals.bmb.a011708. PubMed PMID: 10326282.
627 37. Limthongkul J, Mapratiep N, Apichirapokey S, Suksatu A, Midoeng P, Ubol S. Insect anionic septapeptides suppress DENV
628 replication by activating antiviral cytokines and miRNAs in primary human monocytes. Antiviral research. 2019;168:1-8. Epub
629 2019/05/11. doi: 10.1016/j.antiviral.2019.04.012. PubMed PMID: 31075349.
630 38. Cleaves GR, Ryan TE, Schlesinger RW. Identification and characterization of type 2 dengue virus replicative intermediate
631 and replicative form RNAs. Virology. 1981;111(1):73-83. Epub 1981/05/01. doi: 10.1016/0042-6822(81)90654-1. PubMed PMID:
632 6263011.
633 39. Schlee M. Master sensors of pathogenic RNA - RIG-I like receptors. Immunobiology. 2013;218(11):1322-35. Epub
634 2013/07/31. doi: 10.1016/j.imbio.2013.06.007. PubMed PMID: 23896194; PubMed Central PMCID: PMCPMC7114584.
635 40. Choi KH. The Role of the Stem-Loop A RNA Promoter in Flavivirus Replication. Viruses. 2021;13(6). Epub 2021/07/03. doi:
636 10.3390/v13061107. PubMed PMID: 34207869; PubMed Central PMCID: PMCPMC8226660.
637 41. Wengler G, Wengler G, Gross HJ. Studies on virus-specific nucleic acids synthesized in vertebrate and mosquito cells
638 infected with flaviviruses. Virology. 1978;89(2):423-37. Epub 1978/09/01. doi: 10.1016/0042-6822(78)90185-x. PubMed PMID:
639 568848.
640 42. Sherwood AV, Rivera-Rangel LR, Ryberg LA, Larsen HS, Anker KM, Costa R, et al. Hepatitis C virus RNA is 5'-capped with
641 flavin adenine dinucleotide. Nature. 2023;619(7971):811-8. Epub 2023/07/06. doi: 10.1038/s41586-023-06301-3. PubMed
642 PMID: 37407817.
643 43. Chiang JJ, Sparrer KMJ, van Gent M, Lässig C, Huang T, Osterrieder N, et al. Viral unmasking of cellular 5S rRNA pseudogene
644 transcripts induces RIG-I-mediated immunity. Nature immunology. 2018;19(1):53-62. Epub 2017/11/29. doi:
645 10.1038/s41590-017-0005-y. PubMed PMID: 29180807; PubMed Central PMCID: PMCPMC5815369.
646 44. Runge S, Sparrer KM, Lässig C, Hembach K, Baum A, García-Sastre A, et al. In vivo ligands of MDA5 and RIG-I in measles
647 virus-infected cells. PLoS pathogens. 2014;10(4):e1004081. Epub 2014/04/20. doi: 10.1371/journal.ppat.1004081. PubMed
648 PMID: 24743923; PubMed Central PMCID: PMCPMC3990713.
649 45. Sanchez David RY, Combredet C, Sismeiro O, Dillies MA, Jagla B, Coppée JY, et al. Comparative analysis of viral RNA
650 signatures on different RIG-I-like receptors. eLife. 2016;5:e11275. Epub 2016/03/25. doi: 10.7554/eLife.11275. PubMed PMID:
651 27011352; PubMed Central PMCID: PMCPMC4841775.
652 46. Vabret N, Najburg V, Solovyov A, Gopal R, McClain C, Šulc P, et al. Y RNAs are conserved endogenous RIG-I ligands across
653 RNA virus infection and are targeted by HIV-1. iScience. 2022;25(7):104599. Epub 2022/07/06. doi: 10.1016/j.isci.2022.104599.
654 PubMed PMID: 35789859; PubMed Central PMCID: PMCPMC9250025.
655 47. Zhao Y, Ye X, Dunker W, Song Y, Karijolich J. RIG-I like receptor sensing of host RNAs facilitates the cell-intrinsic immune
656 response to KSHV infection. Nature communications. 2018;9(1):4841. Epub 2018/11/20. doi: 10.1038/s41467-018-07314-7.
657 PubMed PMID: 30451863; PubMed Central PMCID: PMCPMC6242832.
658 48. Paul AV, Wimmer E. Initiation of protein-primed picornavirus RNA synthesis. Virus research. 2015;206:12-26. Epub
659 2015/01/17. doi: 10.1016/j.virusres.2014.12.028. PubMed PMID: 25592245; PubMed Central PMCID: PMCPMC4476921.
660 49. Srikiatkhachorn A, Mathew A, Rothman AL. Immune-mediated cytokine storm and its role in severe dengue. Seminars in
661 immunopathology. 2017;39(5):563-74. Epub 2017/04/13. doi: 10.1007/s00281-017-0625-1. PubMed PMID: 28401256; PubMed
662 Central PMCID: PMCPMC5496927.
663 50. Li L, Gan T, Ma Z, Huang Y, Zhong J. Assessing risk of Bombali virus spillover to humans by mutagenesis analysis of viral
664 glycoprotein. hLife. 2024;2(1):32-42. doi: https://doi.org/10.1016/j.hlife.2023.11.003.
665 51. He Z, Ye S, Xing Y, Jiu Y, Zhong J. UNC93B1 curbs cytosolic DNA signaling by promoting STING degradation. European journal

666 of immunology. 2021;51(7):1672-85. Epub 2021/04/11. doi: 10.1002/eji.202048901. PubMed PMID: 33837956.
667 52. Xie X, Zou J, Zhang X, Zhou Y, Routh AL, Kang C, et al. Dengue NS2A Protein Orchestrates Virus Assembly. Cell host &
668 microbe. 2019;26(5):606-22.e8. Epub 2019/10/22. doi: 10.1016/j.chom.2019.09.015. PubMed PMID: 31631053.
669

671 **Figures and legends**

672 **Fig. 1**

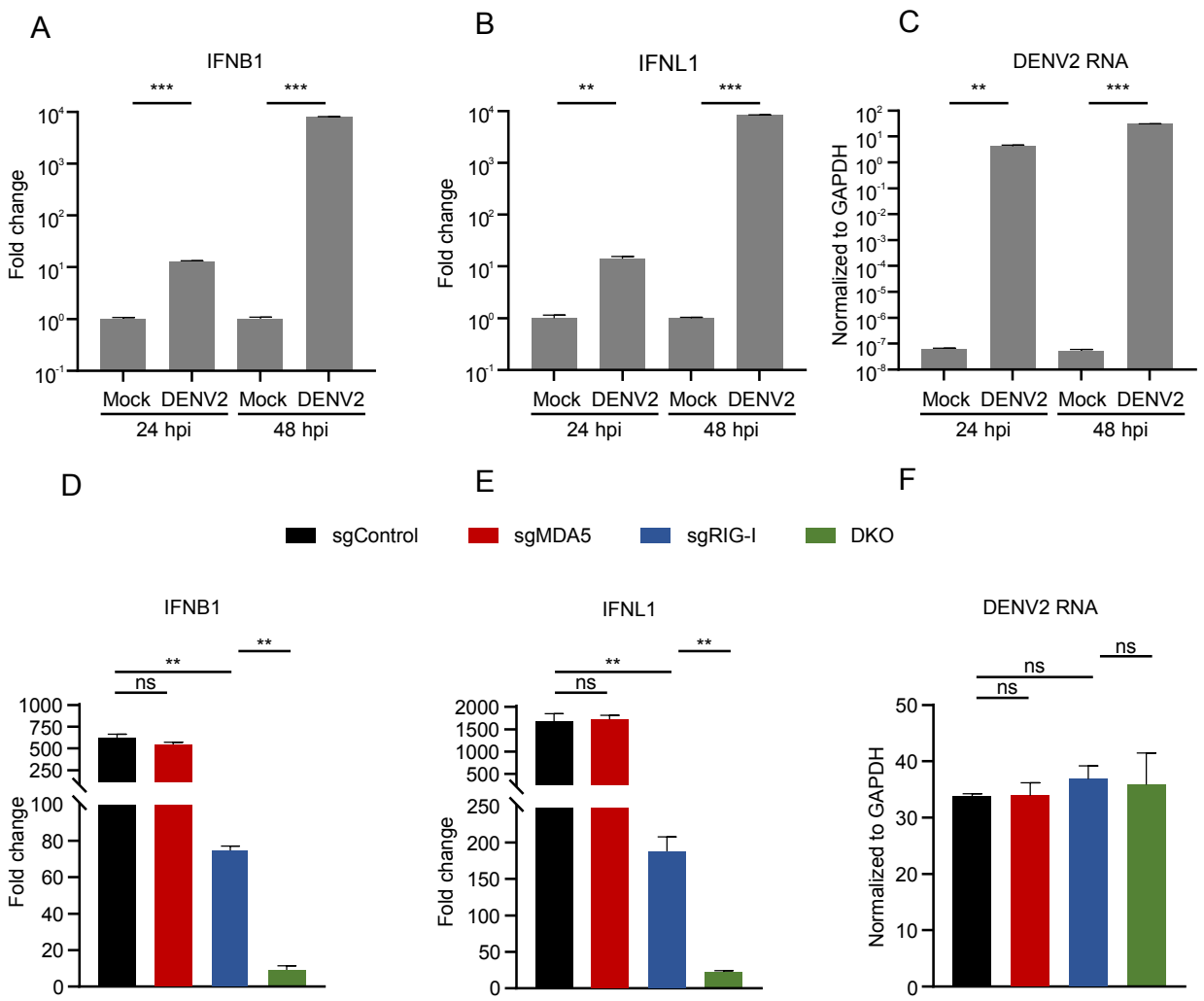

673

674 **Fig. 1. DENV2 infection-induced IFN response is dependent upon both MDA5 and RIG-I, with RIG-I**

675 **playing a predominant role.**

676 (**A-C**) HEK293 cells were infected with DENV2 (MOI=1). Infected cells were analyzed at indicated time

677 points for IFNB1 (**A**), IFNL1 (**B**), DENV2 RNA (**C**) by RT-qPCR. hpi, hours post-infection. (**D-F**) MDA5

678 or RIG-I single knockout cells, as well as DKO HEK293 cells were infected with DENV2 (MOI=1) for 48 h

679 and analyzed by RT-qPCR to detect the mRNA abundance of IFNB1 (**D**), IFNL1 (**E**), DENV2 RNA (**F**).

680 IFNB1 and IFNL1 were normalized against cellular GAPDH mRNA level and expressed as values relative

681 to the mock infection control. DENV2 RNA was expressed as values normalized to the GAPDH mRNA

682 level. The error bars represent standard deviations from two independent experiments. Student's t test was

683 used for statistical analysis. ns, $P>0.05$; **, $p < 0.01$; ***, $p < 0.001$.

685 **Fig. 2**

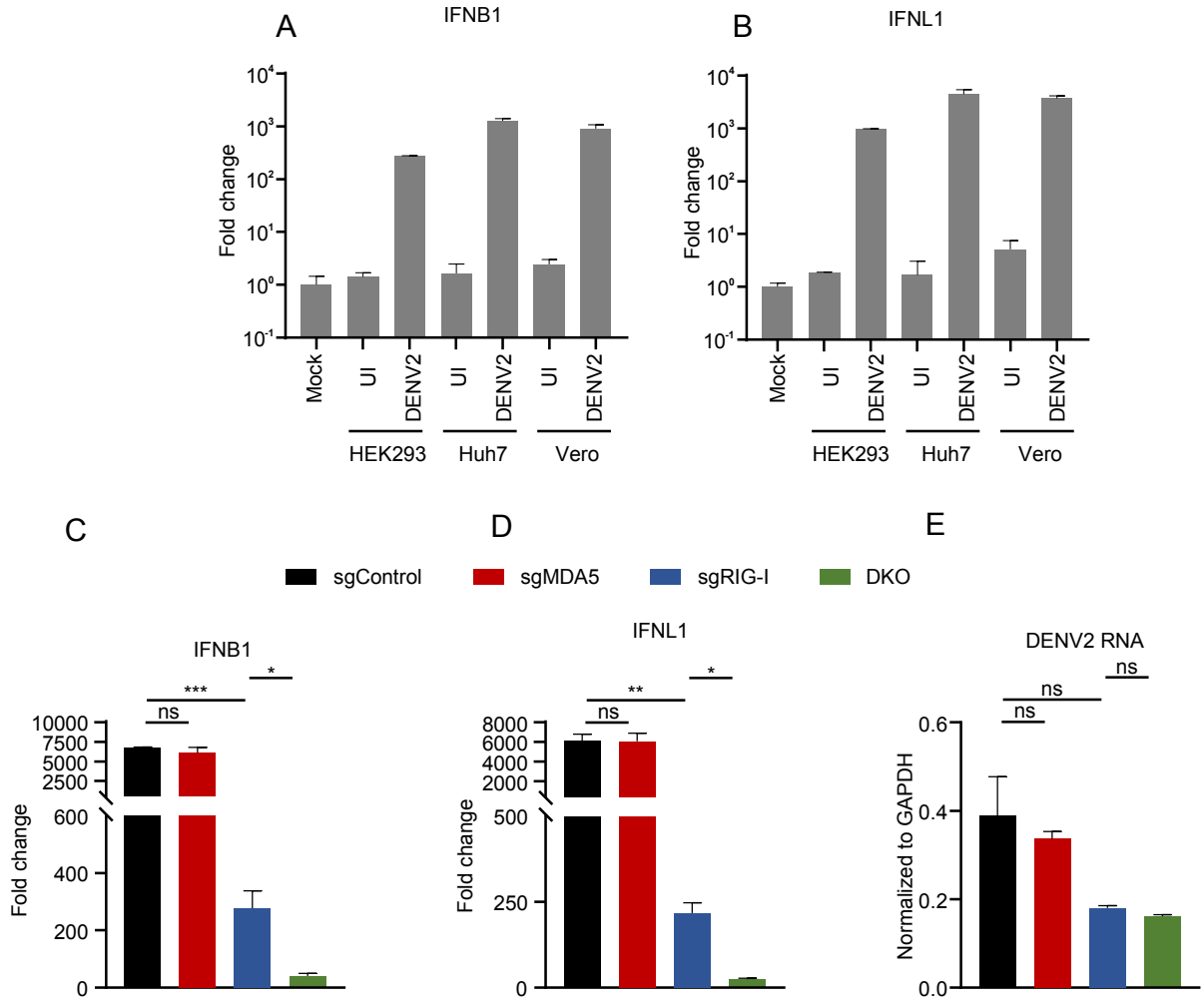

686

687 **Fig. 2. The IFN response stimulated by transfection of DENV2-infected cellular RNA requires both**

688 **RIG-I and MDA5, with RIG-I playing a predominant role.**

689 (**A-B**) HEK293 cells were transfected with the 200 ng of cellular RNA extracted from DENV2 infected or

690 uninfected HEK293, Huh7 and Vero cells for 16 h, and IFNB1 (**A**) and IFNL1 (**B**) mRNA level were

691 determined by RT-qPCR. UI, Uninfected. (**C-E**) RIG-I or MDA5 single knockout cells, as well as DKO

692 HEK293 cells were transfected with 200 ng of DENV2-infected Huh7 cellular RNA for 16 h and analyzed

693 by RT-qPCR to detect the mRNA abundance of IFNB1 (**C**), IFNL1 (**D**), DENV2 RNA (**E**). IFNB1 and

694 IFNL1 were normalized against cellular GAPDH mRNA level and expressed as values relative to the mock

transfection control. DENV2 RNA was expressed as values normalized to the GAPDH mRNA level. The error bars represent standard deviations from two independent experiments. Student's t test was used for statistical analysis for (**C-E**). ns, $P>0.05$; *, $p < 0.05$; **, $p < 0.01$; ***, $p < 0.001$.

699 **Fig. 3**

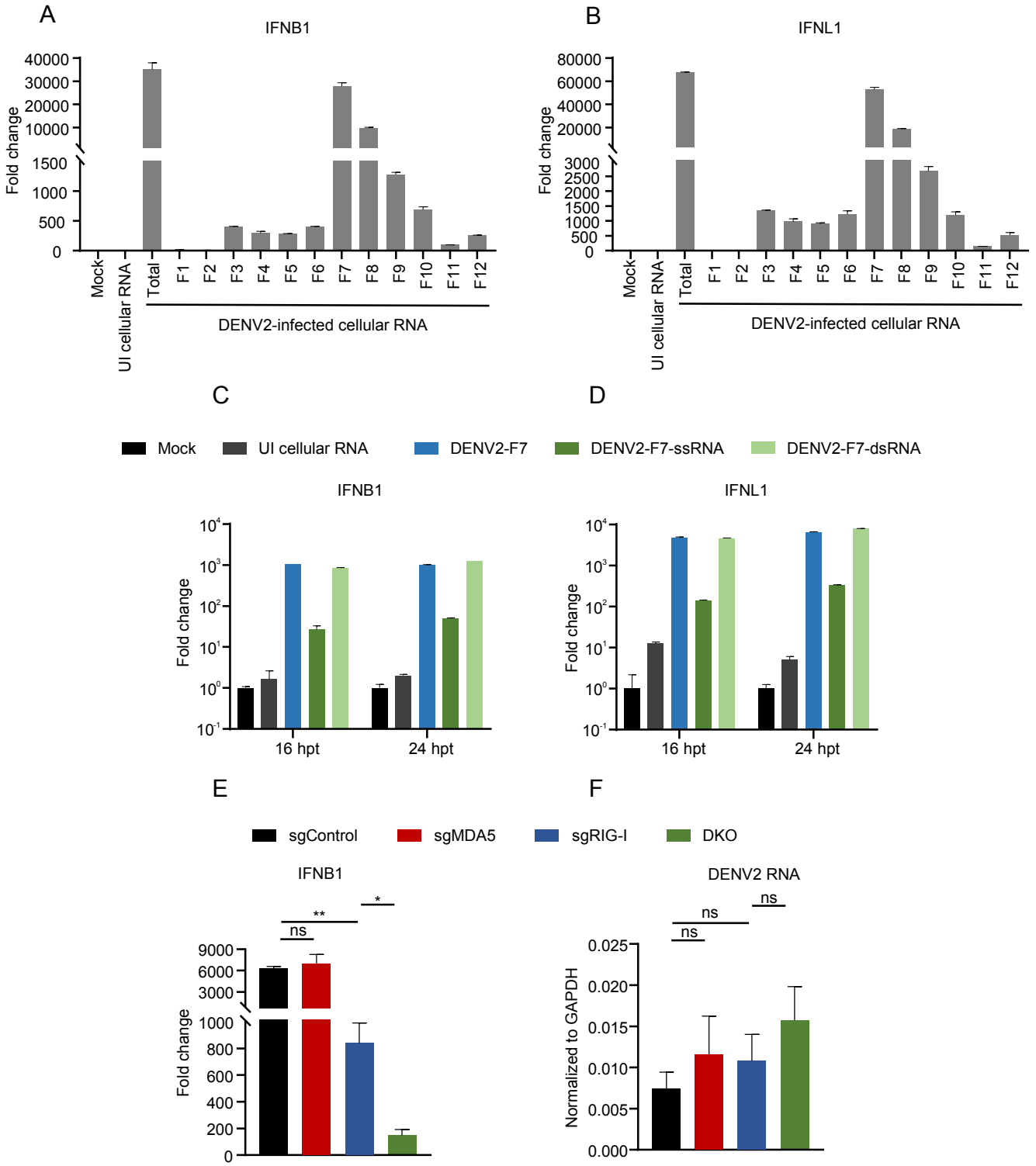

700

701 **Fig. 3. DENV2 PAMPs are enriched through sucrose density gradient centrifugation and LiCl**

702 **differential precipitation.**

703 (**A-B**) HEK293 cells were transfected with equal volume of unfractionated (total) RNA and F1-F12 RNA
704 for 16 h, and IFNB1 (**A**) and IFNL1 (**B**) mRNA levels were determined by RT-qPCR. F1-F12 RNA was
705 stuffed with uninfected Huh7 cellular RNA to make its mass consistent with the unfractionated (total) RNA
706 sample (120 ng). UI, Uninfected. (**C-D**) HEK293 cells were transfected with equal volume of DENV2-F7,
707 DENV2-F7-ssRNA and DENV2-F7-dsRNA. Transfected cells were analyzed at indicated timepoints for
708 IFNB1 (**C**) and IFNL1 (**D**) by RT-qPCR. DENV2-F7 (20 ng), ssRNA and dsRNA were stuffed with 200 ng
709 of uninfected Huh7 cellular RNA to ensure high transfection efficiency. UI, Uninfected. (**E-F**) MDA5 or
710 RIG-I single knockout cells, as well as DKO HEK293 cells were transfected with 0.5 ng of
711 DENV2-F7-dsRNA (stuffed with 200 ng uninfected Huh7 cellular RNA) for 16 h and analyzed by
712 RT-qPCR to detect the mRNA abundance of IFNB1 (**E**) and DENV2 RNA **(F**). IFNB1 and IFNL1 were
713 normalized against cellular GAPDH mRNA level and expressed as values relative to the mock transfection
714 control. DENV2 RNA was expressed as values normalized to the GAPDH mRNA level. The error bars
715 represent standard deviations from two independent experiments. Student's t test was used for statistical
716 analysis for (**E-F**). ns, $P>0.05$; *, $p < 0.05$; **, $p < 0.01$.

717

Fig. 4

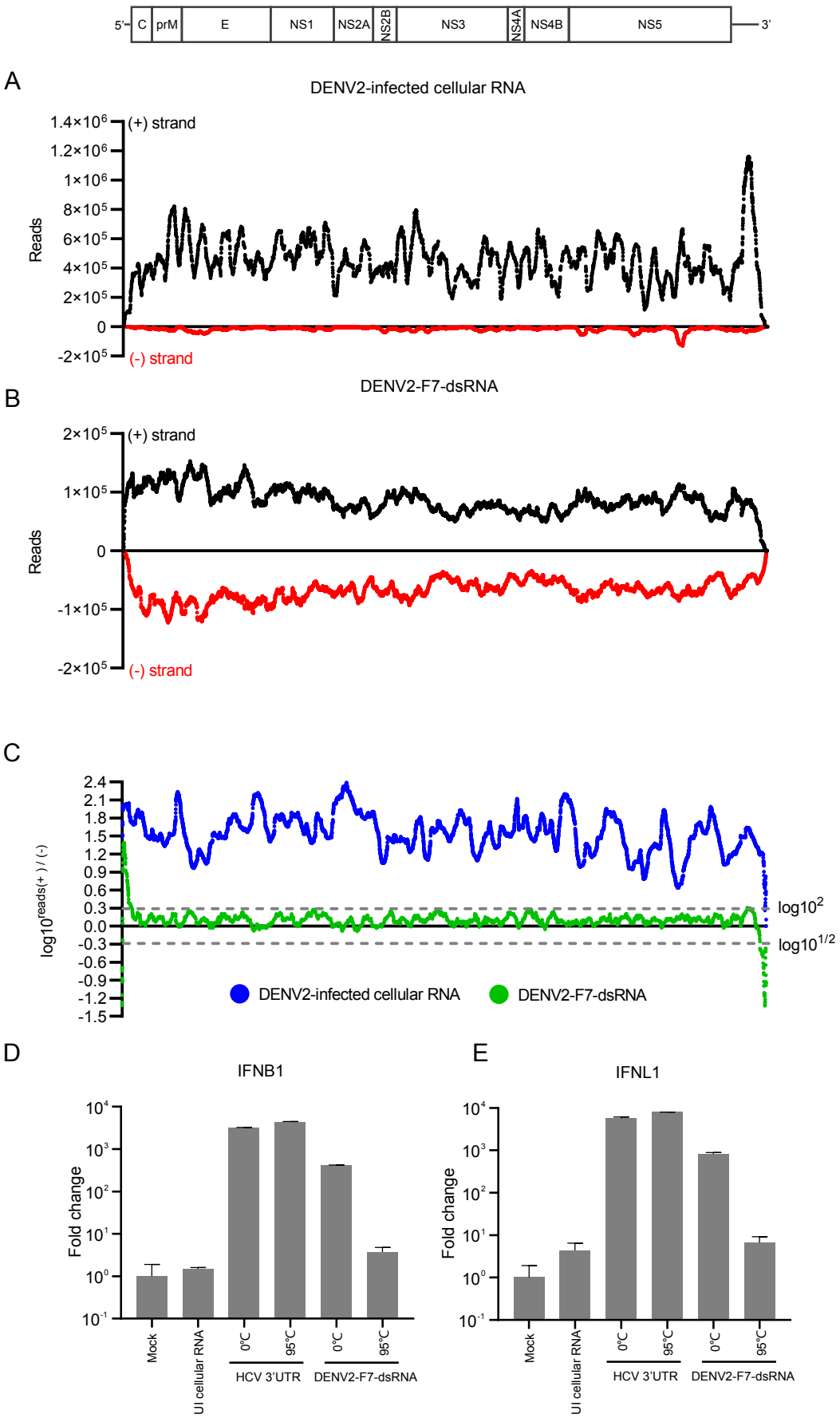
5'
C
prM
E
NS1
NS2A
NS2B
NS3
NS4A
NS4B
NS5
3'
A
DENV2-infected cellular RNA
(+) strand
(-) strand
Reads
B
DENV2-F7-dsRNA
(+) strand
(-) strand
Reads
C
log10reads(+) / (-)
log10^2
log10^1/2
DENV2-infected cellular RNA
DENV2-F7-dsRNA
D
IFNB1
Fold change
Mock
UI cellular RNA
0°C
95°C
0°C
95°C
HCV 3'UTR
DENV2-F7-dsRNA
E
IFNL1
Fold change
Mock
UI cellular RNA
0°C
95°C
0°C
95°C
HCV 3'UTR
DENV2-F7-dsRNA

718 **Fig. 4. DENV2 PAMPs are the DENV2 RF double-stranded RNA.**

719 (**A**) DENV2-infected cellular RNA and (**B**) DENV2-F7-dsRNA samples were subjected to strand-specific
720 RNA-seq analysis. The distribution of read coverage matching DENV2 genomes was represented along the
721 viral genome. The x-axis denoted the nucleotide positions within the DENV2 genome, while the y-axis
722 illustrated the depth of reads aligned to the DENV2 (+) sense RNA in black and the (-) sense RNA in red. (**C**)
723 The ratio was determined by dividing the depth of reads mapped to the (+) sense RNA by the depth of reads
724 mapped to the (-) sense RNA, and the results were represented on a log10 scale. Values between the two
725 gray dotted lines indicated ratios that are within a twofold difference. (**D-E**) 200 ng of HCV 3'UTR and 0.3
726 ng of DENV2-F7-dsRNA were heated at 95°C for 5 minutes and then transfected into HEK293 cells for 16
727 h, and IFNB1 (**D**) and IFNL1 **(E**) were analyzed by RT-qPCR. 200 ng of uninfected cellular Huh7 RNA as a
728 carrier were transfected together with heated DENV2-F7-dsRNA. UI, Uninfected. IFNB1 and IFNL1 were
729 normalized against cellular GAPDH mRNA level and expressed as values relative to the mock transfection
730 control. The error bars represent standard deviations from two measurements.

732 **Fig.5**

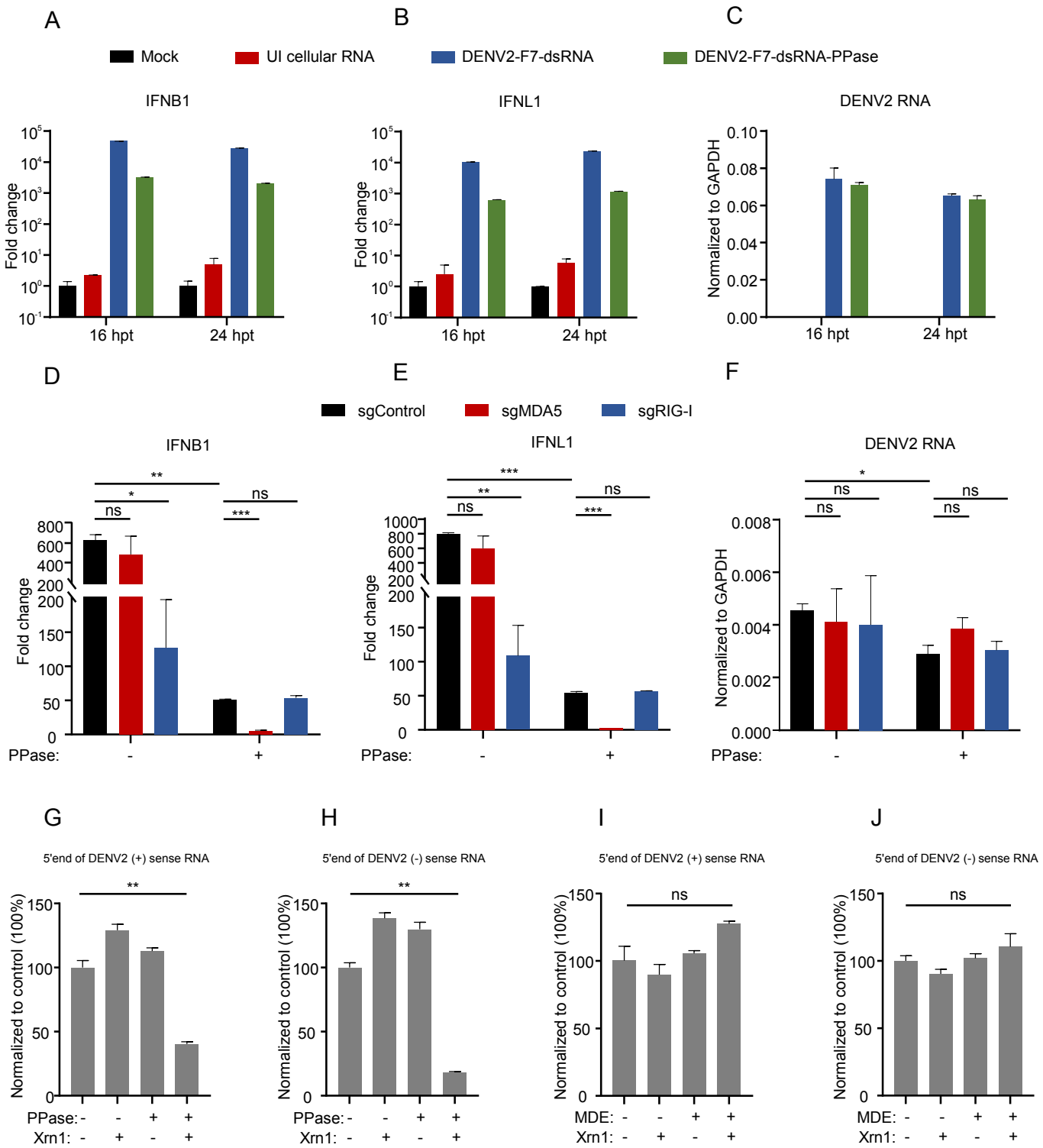

733

734 **Fig. 5. 5'ppp modification of DENV2-F7-dsRNA is essential for RIG-I-mediated signaling, but not for**

735 **MDA5-mediated signaling.**

736 (**A-C**) 0.5 ng of PPase-treated or untreated DENV2-F7-dsRNA was stuffed with 200 ng of uninfected Huh7
737 cellular RNA, and then transfected into HEK293 cells. Transfected cells were analyzed at indicated
738 timepoints for IFNB1 (**A**) and IFNL1 (**B**) and DENV2 RNA **C**) by RT-qPCR. UI, Uninfected. hpt, hours
739 post-transfection. The error bars represent standard deviations from two independent measurements. (**D-F**)
740 RNAs in (**A-C**) were transfected into MDA5 or RIG-I single knockout cells. Transfected cells were
741 analyzed at 16 h for IFNB1 (**D**) and IFNL1 (**E**) and DENV2 RNA (**F**) by RT-qPCR. IFNB1 and IFNL1 were
742 normalized against cellular GAPDH mRNA level and expressed as values relative to the mock transfection
743 control. DENV2 RNA was expressed as values normalized to the GAPDH mRNA level. The error bars
744 represent standard deviations from two independent experiments. (**G-H**) DENV2-F7-dsRNA supplemented
745 with uninfected Huh7 cellular RNA, was subjected to treatment with Xrn1, PPase, or both. DENV2 (+) (**G**)
746 or (-) (**H**) sense RNA were detected by RT-qPCR targeting the 5'end of RNA. **(I-J**) DENV2-F7-dsRNA
747 supplemented with uninfected Huh7 cellular RNA, was subjected to treatment with Xrn1, MDE, or both.
748 DENV2 (+) (**I**) or (-) (**J**) sense RNA were detected by RT-qPCR targeting the 5'end of RNA. The RNA
749 levels were normalized to a control sample. The error bars represent standard deviations from two
750 independent experiments. Student's t test was used for statistical analysis for (**D-J**). ns, $P>0.05$; *, $p < 0.05$;
751 **, $p < 0.01$; ***, $p < 0.001$.

753 **Fig. 6**

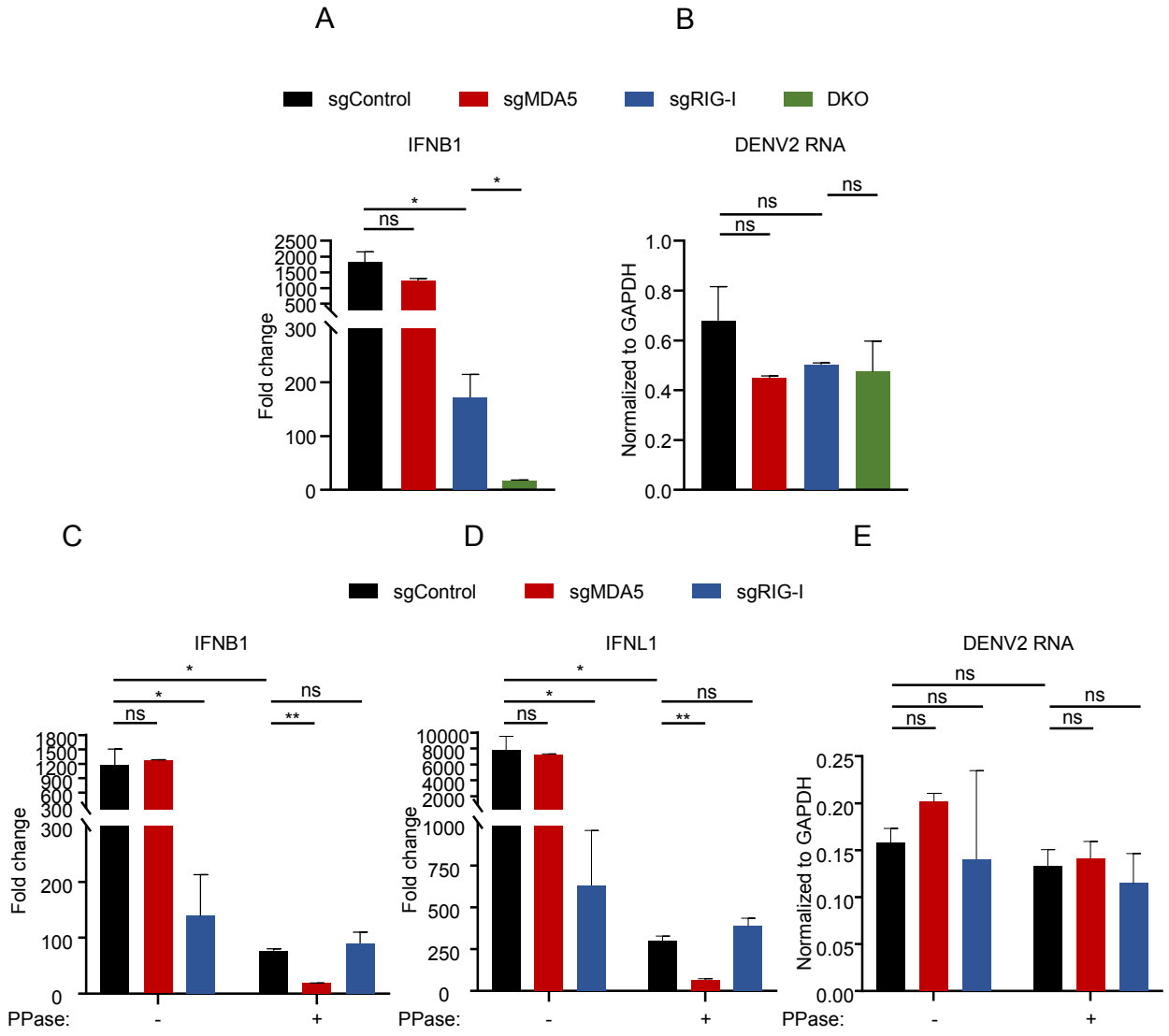

754

755 **Fig. 6. *In vitro* reconstituted DENV2 RF dsRNA exhibits the similar properties to the DENV2 PAMPs.**

756 (**A-B**) RIG-I or MDA5 single knockout cells, as well as DKO HEK293 cells were transfected with 50 ng of

757 reconstituted DENV2 RF dsRNA for 16 h and analyzed by RT-qPCR to detect the mRNA abundance of

758 IFNB1 (**A**), DENV2 RNA (**B**). (**C-E**) 50 ng of reconstituted DENV2 RF dsRNAs were treated with PPase,

759 and then transfected into MDA5 or RIG-I single knockout cells. Transfected cells were analyzed at 16 h

760 post-transfection for IFNB1 (**C**) and IFNL1 (**D**) and DENV2 RNA (**E**) by RT-qPCR. IFNB1 and IFNL1

761 were normalized against cellular GAPDH mRNA level and expressed as values relative to the mock

762 transfection control. DENV2 RNA was expressed as values normalized to the GAPDH mRNA level. The

763 error bars represent standard deviations from two independent experiments. Student's t test was used for

764 statistical analysis. ns, $P>0.05$; *, $p < 0.05$; **, $p < 0.01$.